

Theoretical Estimates of Stellar e^- Captures.

I. The half-life of ${}^7\text{Be}$ in Evolved Stars

S. Simonucci¹, S. Taioli², S. Palmerini³, M. Busso⁴

Received _____; accepted _____

¹Department of Physics, University of Camerino, Italy

¹Istituto Nazionale di Fisica Nucleare, Sezione di Perugia, Italy; stefano.simonucci@unicam.it

²Interdisciplinary Laboratory for Computational Science, FBK-CMM and University of Trento, Italy; taioli@fbk.eu

²Istituto Nazionale di Fisica Nucleare, Sezione di Perugia

²Department of Physics, University of Trento, Italy

²Department of Chemistry, University of Bologna, Italy

³Departamento de Física Teórica y del Cosmos, Universidad de Granada, Spain

⁴Department of Physics, University of Perugia, Italy

⁴Istituto Nazionale di Fisica Nucleare, Sezione di Perugia, Italy

ABSTRACT

The enrichment of Li in the Universe is still unexplained, presenting various puzzles to astrophysics. One open issue is that of obtaining reliable estimates for the rate of e^- -captures on ${}^7\text{Be}$, for T and ρ conditions different from the solar ones. This is of crucial importance to model the Galactic nucleosynthesis of Li. In this framework, we present here a new theoretical method for calculating the e^- -capture rate in conditions typical of evolved stars. Furthermore, we show how our approach compares with state-of-the-art techniques for solar conditions, where various estimates are available. Our computations include: i) “traditional” calculations of the electronic density at the nucleus, to which the e^- -capture rate for ${}^7\text{Be}$ is proportional, for different theoretical approaches including the Thomas–Fermi, Poisson–Boltzmann and Debye–Hückel (DH) models of screening, ii) a new computation, based on a formalism that goes beyond the previous ones, adopting a mean-field “adiabatic” approximation to the scattering process. The results obtained with the new approach as well as with the traditional ones and their differences are discussed in some detail, starting from solar conditions, where our approach and the DH model essentially converge to the same solution. We then analyze the applicability of both our method and the DH model to a rather broad range of T and ρ values, embracing those typical of red giant stars, where both bound and continuum states contribute to the capture. We find that, over a wide region of the parameter space explored, the DH approximation does not really stand, so that the more general method we suggest should be preferred. As a first application, we briefly reanalyze the ${}^7\text{Li}$ abundances in RGB and AGB stars of the Galactic Disk in the light of a revision in the Be-decay only; we however underline that the changes we find in the electron density at the nucleus would induce effects also on the electron screening (for p-captures on Li itself, as well as for other nuclei) so that our new approach might have rather wide astrophysical consequences.

Subject headings: Poisson–Boltzmann, Debye–Hückel, Thomas–Fermi models - first-principles methods - Stars: RGB, AGB - abundances - Nuclear reactions - Nucleosynthesis - Electron screening

1. Introduction

Serious problems affect our understanding of the Li evolution in the Galaxy. Big Bang Nucleosynthesis (BBN: see e.g. Coc & Vangioni 2010, and references therein) predicts a Li abundance higher than observed in extremely metal-poor objects (Bonifacio et al. 2012) and in low-metallicity Main Sequence (MS) stars (Spite and Spite 1982). On the other hand, in the present interstellar medium (ISM) the ${}^7\text{Li}$ abundance is higher even than that expected by BBN (Casuso and Beckmann 2003). As Galactic Cosmic Rays do not produce much ${}^7\text{Li}$ (Fields et al. 1994; Alibés et al. 2002) we should rely on stellar nucleosynthesis for explaining this increase.

${}^7\text{Li}$ is however a very fragile nucleus, so that its photospheric concentration in stars is easily destroyed when convective processes can carry it to moderately high temperatures (a few millions K), where it undergoes proton captures (Boesgaard & Tripicco 1986a). Special conditions are therefore required for Li production, which are limited to a few astrophysical scenarios. These mainly include novae and intermediate mass stars (IMS) undergoing H burning at the base of their envelope through the so-called Hot Bottom Burning process (see e.g. D’Antona & Ventura 2010). In current stellar models for low mass stars (LMS: those with masses below about $2 - 3 M_{\odot}$) Li is instead predicted to be destroyed already in the early phases of evolution, preceding the MS (Pinsonneault 1997; Sestito et al. 2006). In stars of mass lower than solar, whose convective envelopes remain large even during the MS, Li destruction continues through this stage; for higher masses, instead, it is predicted that external convection shrinks and does not include any more zones hot enough to affect Li. Contrary to these model expectations, observations of the Sun and of solar-like stars reveal that they undergo extensive Li-depleting processes during central hydrogen burning. One of the consequences is that the solar photosphere is about 100 times less Li-rich than meteorites (Asplund et al. 2009). Li-destruction processes are known to occur also

at intermediate effective temperatures, in MS stars of the Galactic disc, generating the so-called *Li-dip* (see e.g. Boesgaard & Tripicco 1986b; Balachandran 1995; Boesgaard et al. 1998).

The above phenomena, unexpected from canonical stellar models, have been interpreted (sometimes only qualitatively) in terms of mixing episodes of a nature different from pure convection (Michaud 1986; Michaud & Charbonnau 1991), often attributed to rotationally-induced effects (Charbonnel & Lagarde 2010), atomic diffusion, or magnetic dynamo processes (Eggenberger et al. 2010), like those observed in active stars (Andrews et al. 1988). However, the very large Li destruction in the Sun and in other main sequence stars is still not accounted for in detail, being too small in the models. In more advanced stages, i.e. along the Red Giant Branch (hereafter RGB) and along the Asymptotic Giant Branch (hereafter AGB) similar phenomena must be active (Palmerini et al. 2011a; Maiorca et al. 2012), perhaps again related to magnetic effects (Busso et al. 2007; Nordhaus et al. 2008; Denissenkov et al. 2009). The consequence is that, in most evolved stars, Li is further depleted as compared to MS stages (see e.g. Palmerini et al. 2011b, and references quoted therein).

At odds with our need for finding sites where Li is produced in stars, only few red giants ($\sim 2\%$) show Li enhancement at their photosphere (see e.g. Brown 1987; Charbonnel & Balachandran 2000; Kumar et al. 2011; Uttenthaler & Lebzelter 2010; Lebzelter et al. 2012). Their abundances might in principle be produced by coupled mixing and nucleosynthesis episodes, in which the depletion of Li by downward diffusion is over-compensated by an upward transport of ${}^7\text{Be}$ from burning regions, at a fast enough pace that it survives destruction by p and e^- captures, reaches the stellar envelope and finally decays there, reproducing Li. The situation is however far from being clear (Charbonnel & Lagarde 2010; Palmerini et al. 2011b). Quantitative modeling is in

particular hampered by a poor knowledge of how the rate of Be decay changes in the rapidly varying conditions below the envelopes of red giants. In fact, extrapolations of this rate from the works done for the Sun (Bahcall 1962; Iben et al. 1967; Bahcall & Moeller 1969) are extremely insecure, due the ambient conditions of H burning in evolved stars, which are very different from solar. Indeed, in the layers above the H-burning shell of a red giant the temperature (T) spans a range from 70-80 MK down to a few MK, while the density (ρ) is lower than in the solar center from one to five orders of magnitudes.

In general, the pioneering works of the sixties for the Sun were performed considering the ionization degree of Be through the Saha equation, and including the contribution of free electrons on the assumption that inside a Debye radius around a Be nucleus they behave as a Maxwellian gas, thus following a treatment of the Coulomb screening in the plasma originally due to Debye and Hückel (Debye & Hückel 1923). Although more recent and general approaches do exist (Gruzinov & Bahcall 1997; Brown & Sawyer 1997; Sawyer 2011) sometimes demonstrating the limits of the Debye–Hückel (hereafter DH) approximation (Johnson et al. 1992), they maintain a treatment similar to the Born-Oppenheimer approach, where the electronic response is considered to be much faster than the ionic one. These works almost invariably find for the Sun results very similar to those of the classical studies cited above, but they do not consider the physical conditions prevailing in evolved stars.

It has to be further noted that, at the high temperatures of shell H-burning in red giants, recombination might occur in states that are highly excited and very close to each other. In such conditions, the Born-Oppenheimer approach is questionable; moreover, the conditions for the classical DH approximation often do not actually hold (see next sections) and one does not know whether this introduces small or large deviations in the capture rate.

We decided therefore to explore the problem of e^- captures on ${}^7\text{Be}$ for the typical

T and ρ values of H-burning layers in evolved stars, both following the traditional DH approach and introducing a new treatment, in which the assumption that electrons follow a Maxwell-Boltzmann energy distribution is relaxed (considering them, more generally, as a Fermi gas) and in which a mean-field adiabatic approximation to the scattering process is used. The primary scope is to provide the missing weak-interaction input data for Li nucleosynthesis calculations, clarifying whether such data can be deduced in the traditional way or not. Subsequently, we also plan to apply our results to a re-evaluation of the problem of electron screening in stellar plasmas (see some comments on that issue in sections 3.1 and 5).

We remind that other cases exist, involving nuclei heavier than Li, in which the predictions of nucleosynthesis are still unreliable for the lack of knowledge about the dependence of electron captures on the ambient conditions, during the transport of newly produced nuclei to the stellar surface. Crucial isotopes subject to these uncertainties are, e.g., ^{41}Ca and ^{205}Pb , which are important clocks for dating the latest nucleosynthesis processes before the contraction of the Solar Nebula (see Busso et al. 2003; Busso 2011, and references therein). If one considers also β decays, then it turns out that several reaction branchings along the s -process path are still affected by our poor knowledge of weak interactions in stars, in contrast with the high accuracy of the competing neutron-capture processes.

In general, a better knowledge of radioactive decays would be relevant for a large number of physical problems, well beyond the borders of stellar astrophysics. Accurate decay rates are e.g. of paramount importance in Earth and Planetary sciences, in order to date geological and astronomical processes by estimating the amount of a given long-lived species remaining in a sample (a rock or a stellar photosphere). Furthermore, nuclear decay provides an impressive source of heat in any planetary body, including the Earth.

It is believed that as much as half the heat measured at the Earth surface, corresponding to approximately 21 TW, be due to radioactive processes involving ^{40}K , ^{232}Th , ^{235}U and ^{238}U , occurring both in the crust and in the core (Pollack et al. 1993; Fowler 2005; Lee & Steinle-Neumann 2008). Heating from shorter-lived radioactivities like ^{26}Al is then believed to provide the energy for melting and differentiating the early solid bodies around the Sun (see e.g. Busso 2011, and references therein). In a forthcoming paper our results will therefore be extended to other nuclei and applied to the clarification of a few such problems.

This paper is structured in the following way. In section 2 we provide a general introduction to the current problems of the electron captures on ^7Be . In section 3 we discuss the theoretical framework used for solving the ($^7\text{Be} + e^-$) scattering event, referring to Appendix A for a more detailed technical discussion. In the same section 3 we present calculations of the electron density at the ^7Be nucleus, obtained by applying several models available in the literature (as detailed in Appendix B) and we show comparisons among such values. Section 4 then illustrates in a preliminary way some consequences for the problem of Li production and destruction in evolved stars, while tentative conclusions are drawn in section 5.

2. The electron captures on ^7Be : state-of-the-art.

The driving force responsible for the electron capture decay is the weak nuclear interaction, a process of very short range that was therefore long believed to be insensitive to extra-nuclear factors, notably the chemical environment, the ionization degree, the pressure and temperature conditions. Contrary to this simple view, many authors reported evidence of changes in nuclear decay rates with temperature (Emery 1972; Hahn et al. 1976), pressure (Lee & Steinle-Neumann 2008), and the chemical environment (Ray et al.

2002; Ohtsuki et al. 2007; Morisato et al. 2008), which are believed to be connected to the modification of the electron density at the nucleus, $\rho_e(0)$, induced by the change of these parameters. The rate indeed depends on the s-type atomic-orbital wavefunctions, the only ones with finite density at the nucleus. Therefore, factors affecting this density can appreciably modify the decay rate. Besides T and ρ values, also the pressure, the level of ionization, and the presence of other charged particles, screening the interaction, might in principle be of relevance. On the other side, ab-initio calculations of the radioactive decay rate at room temperature for ${}^7\text{Be}$ (and several other isotopes) performed by Lee & Steinle-Neumann (2008) showed a very small dependence (within $\sim 0.1 - 0.2\%$) on the chemical environment and on the pressure, up to 25 GPa.

Furthermore, very little is still known about decay events that occur at very high T in ionized media for changing ρ , such as those found in stellar interiors, and similar studies are still challenging for theory and intensively debated. The recent recommendations by Adelberger et al. (2011) are mainly based on the work by Bahcall & Moeller (1969) and Iben et al. (1967). In these works a partial ionization of ${}^7\text{Be}$ in the Sun was assumed, thus the rate now currently used includes contributions from both bound and continuum states and the total-to-continuum capture ratio is 1.217. Different results were presented by Shaviv & Shaviv (2003), who assumed that ${}^7\text{Be}$ is fully ionized in the solar plasma; this implied an increase of the ${}^7\text{Be}$ lifetime by ~ 20 to 30% as compared to previous recommendations. An even more complicated situation is depicted by Quarati & Scarfone (2009), who recently found a ${}^7\text{Be}$ lifetime shorter by about 10% , using a modified DH screening potential. The present situation is therefore quite unsatisfactory and the uncertainties affecting Li abundances in stars have to cope also with this poor understanding of the basic nuclear input data.

This is actually the main motivation of our present attempt, as essentially no one of

the existing reaction rate compilations for stellar physics can be safely extrapolated from the Sun to other situations. For example, the rate by Adelberger et al. (2011) is derived from a simple fit over a very small domain of the parameter space, while the formula by Fowler et al. (1975) imposes a specific choice for the density.

In this context, our goal is to lay the foundations of a theoretical and computational method for studying the electron capture and decay rates at high temperature in a density-varying medium, to go beyond the existing treatments. We shall probe its validity through a comparison with more classical approaches, and shall use the results to reconsider briefly the problem of Li production and destruction in red giant stars.

3. Dynamics of electron capture from *ab-initio* calculations: our model

In this section we describe our first-principle approach for computing electron captures over a much wider range of T and ρ than so far possible. These two parameters alter considerably the balance between bound and free electronic states contributing to the capture.

While we believe that our formalism is totally general and can be applied even to other systems, as a test case of our method we will estimate the decay rate of ${}^7\text{Be}$ by electron captures:



${}^7\text{Be}$ can decay into ${}^7\text{Li}$ through different decay channels. In particular, the decay from the ground state of ${}^7\text{Be}$ can occur to both the ground and the first excited state of ${}^7\text{Li}$. Of course the phase space and the kinetic energy of the neutrinos will be different for these two decay paths. At ambient conditions, i.e. for negligible kinetic energy of the impinging electron, ${}^7\text{Be}$ decays in 53 days into the ground state of ${}^7\text{Li}$ ($3/2^-$) for the 89.7% of cases, while for the remaining 10.3% it decays into the first excited state ($1/2^-$), as discussed by

Mathews et al. (1983). The energy of this latter is 477.4 KeV higher than for the ground state. The weak branching ratio (BR) at room temperature is therefore 8.709. By defining Q_0 and Q_1 as the kinetic energies of the neutrinos, escaping respectively from the ${}^7\text{Li}$ nucleus in its ground and in its first excited state, we have $Q_0 = 861.6$ keV and $Q_1 = Q_0 - 477.4 = 384.2$ keV (Fuller & Smith 2010). Being the kinetic energy higher in the first case, the available phase space will be larger. Roughly we can estimate that, at a temperature $T = 10^7$ K, $\text{BR} = 89.7/10.3 \times (Q_0 + kT)^2 / (Q_1 + kT)^2 / (Q_0^2 / Q_1^2) = 8.684$. The percentage variation of the BR due to an increase of the temperature by five orders of magnitude is thus only 0.3%. Of course, even the weak matrix elements will be different for these two channels and this should be in principle taken into account. However, our main goal here is to estimate accurately the total electron capture decay rate, as this is what we need for assessing the astrophysical consequences of our new results. Thus, in the following discussion we shall assume that the decay occurs only to the ground state of ${}^7\text{Li}$.

The framework within which we shall calculate the decay rate is given by the theory of scattering under two potentials: V , representing the screened, short-range Coulomb potential and W , which represents the weak interaction coupling the Coulomb distorted initial state and the final channels. We define $\phi_{i,\mathbf{p}}$ as a free plane-wave, $\phi_{i,\mathbf{k}}^+$ the perturbed ‘in-state’, described by a Coulomb-distorted plus an outgoing spherical wave, $\phi_{f,\mathbf{k}}^-$ and $\psi_{f,\mathbf{k}}^-$ the perturbed ‘out-states’, which describe asymptotically the emission of a neutrino with relative momentum \mathbf{k} , released into the final channel f of the target, respectively with and without the weak coupling. Then we can write the cross section of the electron capture process as:

$$\begin{aligned} \sigma_{i \rightarrow f} &= \int \frac{d^3k}{(2\pi)^3} \frac{2\pi}{v} \left| \langle \psi_{f,\mathbf{k}}^- | W | \phi_{i,\mathbf{p}}^+ \rangle + \langle \phi_{f,\mathbf{k}}^- | V | \phi_{i,\mathbf{p}} \rangle \right|^2 \delta \left(\frac{p^2}{2m_e} + E_i - E_f - ck \right) \\ &= \int \frac{d^3k}{(2\pi)^3} \frac{2\pi}{v} \left| \langle \phi_{f,\mathbf{k}}^- | T_w | \phi_{i,\mathbf{p}}^+ \rangle \right|^2 \delta \left(\frac{p^2}{2m_e} + E_i - E_f - ck \right) \end{aligned} \quad (2)$$

E_i, E_f represent the internal energies of the target (${}^7\text{Be}$) and of the final decay product

(${}^7\text{Li}$), $\mathbf{p} = m_e v$ and \mathbf{k} are the relative electron and neutrino momenta in the initial and final channels, and v is the electron velocity in the initial channel, relative to ${}^7\text{Be}$. In Eq. (2) the matrix element $\langle \phi_{f,\mathbf{k}}^- | V | \phi_{i,\mathbf{p}} \rangle$ must vanish, as the Coulomb interaction does not couple the initial and final decay channels ($\langle \phi_{f,\mathbf{k}}^- | V | \phi_{i,\mathbf{p}} \rangle = 0$). Thus we can define the T -matrix of the weak interaction as

$$\langle \psi_{f,\mathbf{k}}^- | W | \phi_{i,\mathbf{k}}^+ \rangle = \langle \phi_{f,\mathbf{k}}^- | T_W | \phi_{i,\mathbf{k}}^+ \rangle \quad (3)$$

From Eq. (2) one can obtain the electron capture rate by multiplying the cross section for the electron current:

$$\Gamma_{i \rightarrow f} = \int 2\pi \frac{d^3 k}{(2\pi)^3} |\langle \phi_{f,\mathbf{k}}^- | T_w | \phi_{i,\mathbf{p}}^+ \rangle|^2 \delta \left(\frac{p^2}{2m_e} + E_i - E_f - ck \right) \quad (4)$$

The calculation of the nuclear T -matrix elements, particularly with the inclusion of the $p^2/2m_e$ dependence, is very difficult from first-principles and is out of the scope of this paper. Indeed $p^2/2m_e$ depends on the temperature of the system. However, the full calculation is not needed in our case, and two approximations will enable us to simplify the equations without sacrificing accuracy. Firstly, we will neglect the dependence on the temperature of this matrix element, and consider only one initial state. This approximation is motivated by the fact that the first nuclear excited state of ${}^7\text{Be}$ is at 429.2 keV above the ground state (Fuller & Smith 2010), corresponding to a temperature of 5×10^9 K, larger by factors of 50 to 100 with respect to the maximum values found during H-shell burning in the RGB or AGB phases.

The second approximation is to model the weak interaction, owing to its very short-range nature, by a Fermi contact interaction $T_W \propto \delta(\mathbf{r})$, independent of the neutrino momentum \mathbf{k} . By integrating out in \mathbf{k} using the latter assumption:

$$\begin{aligned} \Gamma_{i \rightarrow f} &= \frac{\bar{k}^2}{\pi c} |t_{f,i} \langle i, 0 | \phi_{i,\mathbf{p}}^+(0) \rangle|^2 = \frac{1}{\pi c^3} |t_{f,i}|^2 \langle i, 0 | \phi_{i,\mathbf{p}}^+ \rangle \left(\frac{p^2}{2m_e} + E_i - E_f \right)^2 \langle \phi_{i,\mathbf{p}}^+ | i, 0 \rangle \\ &= \frac{1}{\pi c^3} |t_{f,i}|^2 \langle i, 0 | \phi_{i,\mathbf{p}}^+ \rangle (H_0 + V + E_i - E_f)^2 \langle \phi_{i,\mathbf{p}}^+ | i, 0 \rangle \end{aligned} \quad (5)$$

where $\bar{k} = \frac{1}{c} \left(\frac{p^2}{2m_e} + E_i - E_f \right)$ and $\langle \phi_{i,\mathbf{p}}^+ | i, 0 \rangle$ is the electron wavefunction representation at the Be nucleus. We will assume that the nuclear T -matrix elements $t_{f,i}$ are known and equal to those measured on the Earth. The assumptions of Eq. (5) imply that the electron capture can be modeled as a ${}^7\text{Be}-e^-$ two-body scattering process at a given relative electron momentum p , and that the rate is proportional to the electron density at the nucleus $\rho_e(0)$, which is screened and modified by the presence of the surrounding particles.

Our model system of the hot plasma, for different conditions of T and ρ , is represented by a homogeneous Fermi gas composed by ${}^7\text{Be}$ atoms surrounded by N_p protons (hydrogen nuclei) and N_e electrons. The presence of other particles, such as helium, will be neglected in the following discussion and in the stellar decay rate calculation, unless otherwise stated. However, the generalization of our method to include several species is straightforward.

An *exact, ab-initio* calculation of the electron capture rate would be extremely complex, due to the many-body nature of the scattering, and one needs to introduce some further approximations. The first step of our method is thus the formal reduction of this complicated many-body problem to a screened two-body scattering problem, by using an “adiabatic” factorization of the eigenfunctions, resembling the widely known Born-Oppenheimer (BO) approximation adopted in standard electronic structure methods. This goal is reached by fixing the reference frame into the ${}^7\text{Be}$ nucleus and by writing the different parts of the Hamiltonian in this non-inertial frame (we remember that the ${}^7\text{Be}$ nucleus is in principle free to move around). In every sense this is only a coordinate transformation. However, as in classical mechanics, the consequence of using a non-inertial frame will bring about some complicacy (apparent forces), e.g. in this case we will have a two-body kinetic energy operator. In the appendix we describe the mathematical details of this derivation, from which we obtain that the many-body scattering Hamiltonian in the

coordinate system relative to the ${}^7\text{Be}$ nucleus can be written as:

$$\begin{aligned}
H = & \sum_{j=1}^{N_e} \left(-\frac{1}{2m_e} - \frac{1}{2M_{Be}} \right) \nabla_{e,j}'^2 + \sum_{J=1}^{N_p} \left(-\frac{1}{2m_p} - \frac{1}{2M_{Be}} \right) \nabla_{p,J}'^2 - \sum_{j=1}^{N_e} \frac{Z_{Be}}{|\mathbf{r}'_{e,j}|} + \sum_{J=1}^{N_p} \frac{Z_{Be}}{|\mathbf{R}'_{p,J}|} \\
& - \sum_{j=1}^{N_e} \sum_{J=1}^{N_p} \frac{1}{|\mathbf{r}'_{e,j} - \mathbf{R}'_{p,J}|} + \sum_{j=1}^{N_e} \sum_{k=j+1}^{N_e} \frac{1}{|\mathbf{r}'_{e,j} - \mathbf{r}'_{e,k}|} + \sum_{J=1}^{N_p} \sum_{K=J+1}^{N_p} \frac{1}{|\mathbf{R}'_{p,J} - \mathbf{R}'_{p,K}|} - \frac{1}{2M_{Be}} \nabla_{Be}'^2 \\
& - \sum_{\substack{J,J'=1 \\ J \neq J'}}^{N_p} \left(\frac{1}{M_{Be}} \nabla'_{p,J} \cdot \nabla'_{p,J'} \right) - \sum_{\substack{j,j'=1 \\ j \neq j'}}^{N_e} \left(\frac{1}{M_{Be}} \nabla'_{e,j} \cdot \nabla'_{e,j'} \right) - \frac{1}{M_{Be}} \sum_{j=1}^{N_e} \sum_{J=1}^{N_p} \nabla'_{p,J} \cdot \nabla'_{e,j} \\
& + \sum_{j=1}^{N_e} \left(\frac{1}{M_{Be}} \nabla'_{e,j} \cdot \nabla'_{Be} \right) + \sum_{J=1}^{N_p} \left(\frac{1}{M_{Be}} \nabla'_{p,J} \cdot \nabla'_{Be} \right)
\end{aligned} \tag{6}$$

where, in order of appearance, one has the electron and proton kinetic energies, the electron-Be and proton-Be potential energies, the electron-proton, electron-electron, proton-proton interaction, the Be kinetic energy and, finally, terms coupling the different particle species. In the inter-particle coupling terms, resulting from our coordinate transformation, $\{\mathbf{r}'_{e,j}, \mathbf{R}'_{p,J}\}$ identify the coordinates of the j -electron and J -proton relative to the ${}^7\text{Be}$ coordinate, $\mathbf{R}_{Be} = \mathbf{R}'_{Be}$.

We then look for separable eigensolutions of the form:

$$\Psi(\mathbf{R}'_{Be}, \{\mathbf{r}'_e\}, \{\mathbf{R}'_p\}) = \chi(\mathbf{R}'_{Be}) \Phi(\{\mathbf{r}'_e\}, \{\mathbf{R}'_p\}) \tag{7}$$

$$\nabla'_{Be} \chi(\mathbf{R}'_{Be}) = \mathbf{k} \chi(\mathbf{R}'_{Be}) \tag{8}$$

This wavefunction factorization differs from the usual formulation of the BO approximation in two ways. At variance with the BO approximation, the function $\Phi(\{\mathbf{r}'_e\}, \{\mathbf{R}'_p\})$ in Eq. (7), written in the ${}^7\text{Be}$ reference system, does not depend parametrically on the ${}^7\text{Be}$ coordinates and thus needs to be calculated only once. Furthermore, the BO approximation is applicable only when the electronic potential energy surfaces are well separated. These are not our conditions, as the electrons, for T and ρ values pertinent to the burning regions

of stars, occupy either highly excited states of the ${}^7\text{Be}$ atom or continuum orbits. Thus, we are out of reach of the BO scheme, which cannot be rigorously applied.

However, it can be shown that the last two coupling terms in Eq. (6), which are crucial for the application of our mean-field treatment of the many-body interaction, can be neglected. In Appendix A we provide a detailed explanation of the conditions where this approximation can be used.

We notice that, by introducing the two-body framework and the relative coordinate system, we can achieve two important results. The first one is that in our approach the ${}^7\text{Be}$ nucleus is in principle free to move around (thus overcoming the limitations of the Born-Oppenheimer scheme), even though in general its motion is strongly limited by the presence of other particles; the second one is that, by neglecting the two last terms of Eq. (6), the two-body electron- ${}^7\text{Be}$ density-matrix can be factorized as the product of two one-body density-matrices and thus it is possible to introduce different schemes of approximations to the many-body interaction, including the Hartree-Fock's one (hereafter HF). Therefore, the screening brought about by all the interacting fermions of the surrounding environment, which modifies the two-body electron- ${}^7\text{Be}$ scattering and thus the electron-capture rate, can be now taken into account, using standard many-body techniques.

3.1. Screening at different levels of accuracy: Thomas-Fermi, Poisson-Boltzmann and Debye-Hückel

While the importance of the screening for the assessment of the electron-capture rate is well understood, the approaches used so far are all based on the DH approximation; thus, their reliability is not a priori guaranteed in every situation. Within this approximation Iben et al. (1967), for example, realized that, in solar conditions, the electron density at

the nucleus is reduced by the electronic screening for both bound and continuum electrons. Gruzinov & Bahcall (1997) further improved this model by integrating the density-matrix equation to treat on similar grounds the bound and continuum electrons, and by including via a Monte-Carlo approach non-spherical charge fluctuations induced by the small number of ions within the radius λ_D of a Debye sphere.

Despite these improvements, the conclusions drawn by these works rely on the assumption that the hot plasma can be modeled as a classical non-interacting electron gas, screened by using the DH model, in thermodynamic equilibrium with a heat bath at absolute temperature T . The range of applicability of this approximation is based on both classical and statistical considerations: for the former ones, we need a large number of electrons and a high temperature; for the latter ones, we require a smooth change of the potential over a characteristic distance (λ_D), which is large as compared to the thermal De-Broglie wave-length of the electrons (λ_{DB}). However, in the solar case, where $T \simeq 16 \times 10^6 K$, $\rho = 150 g/cm^3$, we have, for the electrons, $\lambda_D = 0.407$, $\lambda_{DB} = 0.352$ a.u.. The conditions are therefore, already for our Sun, at the limits of validity of the classical (Maxwell-Boltzmann) gas approximation. Over the more extended range of parameters characterizing the radiative layers above the H-shell in a red giant (down to $T \simeq 2.0 \times 10^6 K$) the application of the Maxwell-Boltzmann distribution might no longer be justified.

We underline that the simple DH approach, commonly used in the literature so far, can actually be derived as a two-step approximation of the more general Thomas-Fermi (hereafter TF) model, by using the linearized Maxwell-Boltzmann distribution. (In Appendix B we provide a detailed discussion of the DH treatment).

Hence we can compute the crucial parameter, i.e. the electron density at the Be nucleus $\rho_e(0)$, at different levels of approximation, in order to disentangle the differences introduced in the results by the various approaches. In Table 1 we report the results of

such calculations, adopting as an example the solar conditions. We underline that $\rho_e(0)$ is directly related to the electron-capture rate.

In the above calculations, the plasma was modelled by a ${}^7\text{Be}$ nucleus surrounded by a Fermi gas occupying an infinite volume and helium was explicitly included. One can see that both the classical Poisson–Boltzmann approach (PB) and the DH approximation give sizeable different results (of the order of 38% and 6% respectively) with respect to the TF approximation, already for solar conditions. The change becomes even larger when we use our more general method, based on the HF approximation, which we will discuss in the next section. (Surprisingly, the DH approximation is closer to the HF and TF results than the PB case, from which it is derived by linearization).

Table 1

$\rho_{HF}(0)$	$\rho_{TF}(0)$	$\rho_{PB}(0)$	$\rho_{DH}(0)$
16.320 ± 0.020	16.135 ± 0.025	14.870 ± 0.020	16.085 ± 0.025

Table 1: Values (in atomic units) of the electron density at the Be nucleus $\rho_e(0)$ for different levels of the theory (HF=Hartree–Fock, TF=Thomas–Fermi, PB=Poisson–Boltzmann, DH=Debye–Hückel) for solar conditions ($T = 16\text{MK}$). The conditions at which we performed the calculations are $T = 15.67\text{MK}$, $\rho=152.9 \text{ g/cm}^3$, $X_{\text{H}} = 0.34608$, $X_{\text{He}} = 0.63368$.

Even more important, one must underline that the PB and DH approximations do not hold outside the conditions of the solar nucleus. This is true, in particular, at lower temperatures and densities, where a large part of the Li production occurs (because the competing p-captures on ${}^7\text{Be}$ become ineffective). In order to check this point, we performed the calculations of the the electron density at the Be nucleus for all the previously discussed approaches over a wide range of T and ρ conditions. The results are reported in Table 2, where T is in units of 10^6K and ρ in g/cm^3 . Values at the left of the vertical bar (|) represent the electron density at the nucleus $\rho_e(0)$, while those at the right represent $\rho_e(0)$ multiplied by $(1 + p^2/2m)/(E_i - E_f)$ (see Eq. 5), to which the capture rate is proportional.

The Debye radius λ_D and the De-Broglie wavelength λ_{DB} for electrons (e^-) and protons (p) are given in atomic units.

From the analysis of the electron density at the nucleus $\rho_e(0)$ for the different approximations, it is clear that, when we are out of reach of the DH approximation ($\lambda_D \leq \lambda_{DB}$), the values calculated using this model may differ by more than 30% from the HF values. In particular, we underline that, except for very high temperatures, the PB approximation is extremely unreliable, while over the whole considered range of T and ρ values, the TF model systematically underestimates the density at the nucleus $\rho_e(0)$. At variance with this, the DH model, except for low temperatures ($T \leq 10^6$ K), seems to partially correct the wrong behavior of the PB approximation, but not in a systematic way. This is due to the fact that the electron density at the nucleus $\rho_e(0)$ is finite for the DH model, while it is infinite for the Boltzmann approximation (in the HF method the density is always finite, due to the fact that in this case the electronic wavefunction is finite at the nucleus). It is thus evident that the DH model fails in capturing the electron screening properties over a portion of the parameter space that is very important for Li nucleosynthesis and, if one is to assess accurately the electron-capture rate of ${}^7\text{Be}$ in that region, it is necessary to go beyond this approach.

We notice that the issue at stake here is not only a better estimate of weak interactions. If the traditional methods underestimate the electron density over a considerable part of the conditions typical of H-burning in Red Giants, as it seems to be the case, then this implies that they also underestimate the effect of electrons in screening strong interactions. In the case we discuss here (Li production and destruction) our next step will therefore be a re-evaluation of electron screening for proton captures on ${}^7\text{Li}$, which occur down to very low temperatures (few 10^6K). It is well known that the huge destruction of Li in the Sun is still unaccounted for quantitatively, being too small in the models, so that a more effective

process of proton captures on Li, induced by an increased estimate of the electron density and of its screening of the Coulomb barrier, might have important consequences on solar physics and on our understanding of nucleosynthesis in general.

At high temperature and high density ($T \geq 10^7$ K, $\rho \geq 100$ g/cm³) the approaches discussed so far (with the exception of the purely classic PB treatment) become essentially equivalent to one another, as shown in Table 1; in particular, the values of the electron density at the Be nucleus produced by our new method and the one from the DH approximation differ by less than 1.5% (see Table 1, column 1 and 4).

3.2. Calculations of an accurate decay rate from first principles

In order to apply our model Hamiltonian, Eq. (6), to the calculation of the capture rate over a wider range of T and ρ values than so far possible, we need to develop new tools, suitable to go beyond the DH approximation and capable of treating accurately the electronic screening for both bound and continuum electrons. We will then use the new estimates for interpreting the observational data.

In our approach, the Coulomb screening is calculated using a temperature-dependent HF method, within the canonical ensemble, by populating both the ground-state and excited-state atomic orbitals via a Fermi-Dirac distribution. In our treatment, we will neglect the electron-proton pair-formation at low temperature ($T < 10^6$ K). Our method can be outlined as follows. i) We assume that the decay rate is proportional to $\rho_e(0)$ calculated by solving self-consistently a system of coupled HF equations for protons and electrons in the electrostatic field of a ⁷Be nucleus at the origin of the coordinate system. ii) The coupling is given by the self-consistent Hartree term, describing the Coulomb interaction between the two fermionic species. iii) The chemical potentials of protons and electrons are chosen in such a way that the system is neutral far from the ⁷Be atom. iv)

Within this framework, the scattering of ${}^7\text{Be}$ with protons and electrons is a two-body interaction, with the remaining particles acting as a mean-field.

The first step in the above list consists in solving self-consistently the equations for the electron charge density ρ and the potential V to calculate the electron-capture rate. The HF equations for this problem read:

$$-\frac{1}{2m_j}\nabla^2\psi_{j,\alpha\sigma_e\tau_{Be}n}(\mathbf{r}) + V_j^{ext}(\mathbf{r})\psi_{j,\alpha\sigma_e\tau_{Be}n}(\mathbf{r}) - \mu_j\psi_{j,\alpha\sigma_e\tau_{Be}n}(\mathbf{r}) \quad (9)$$

$$+ \sum_{\beta\sigma'_e\tau'_{Be}} \int d\mathbf{r}' V_{j,\alpha\sigma_e\tau_{Be}\beta\sigma'_e\tau'_{Be}}^{HF}(\mathbf{r}, \mathbf{r}')\psi_{j,\beta\sigma'_e\tau'_{Be}n}(\mathbf{r}') = \epsilon_{j,n}\psi_{j,\alpha\sigma_e\tau_{Be}n}(\mathbf{r})$$

$$\rho_{j,\alpha\sigma_e\tau_{Be}\alpha'\sigma'_e\tau'_{Be}}(\mathbf{r}, \mathbf{r}') = \sum_n \frac{1}{e^{\frac{\epsilon_{j,n}}{kT}} + 1} \psi_{j,\alpha\sigma_e\tau_{Be}n}(\mathbf{r})\psi_{j,\alpha'\sigma'_e\tau'_{Be}n}(\mathbf{r}') \quad (10)$$

$$V_{j,\alpha\sigma_e\tau_{Be}\alpha'\sigma'_e\tau'_{Be}}^{HF}(\mathbf{r}, \mathbf{r}') = \delta(\mathbf{r} - \mathbf{r}') \sum_{j'\beta\beta'} \int d\mathbf{s} \frac{Z_j Z_{j'}}{|\mathbf{r} - \mathbf{s}|} \delta_{\sigma_e\sigma'_e} \delta_{\tau_{Be}\tau'_{Be}} \rho_{j',\beta\sigma''_e\tau''_{Be}\beta\sigma''_e\tau''_{Be}}(\mathbf{s}, \mathbf{s}) \quad (11)$$

$$- \frac{Z_j^2}{|\mathbf{r} - \mathbf{r}'|} \delta_{\alpha\alpha'} \delta_{\sigma_e\sigma'_e} \delta_{\tau_{Be}\tau'_{Be}} \rho_{j,\alpha\sigma_e\tau_{Be}\alpha'\sigma'_e\tau'_{Be}}(\mathbf{r}, \mathbf{r}')$$

In Eqs. (9, 10, 11), σ_e ($\frac{1}{2}$) and τ_{Be} ($\frac{3}{2}$) are the electronic and nuclear spins, while α and β represent all the other quantum numbers. The index j runs over all the fermionic particle types. The self-consistent HF potential is used in Eq. (5), along with the external potential, $V = V_{HF} + V_{ext}$, to calculate the (static exchange) electron-capture decay rate.

In order to be complete, the above treatment of the many-body interaction needs to include the electron and proton continuum states, as the capture can occur from the continuum orbitals and, at high T , the plasma is from partially to totally ionized. To include the continuum states in the HF equations, we used the theory of projected potentials, developed for the calculation of the electronic emission spectra from solids (Taioli et al. 2009a,b, 2010). Within this theory, while the Coulomb interaction among the particles (see Eq. 6) is projected onto the Hilbert space spanned by a basis set,

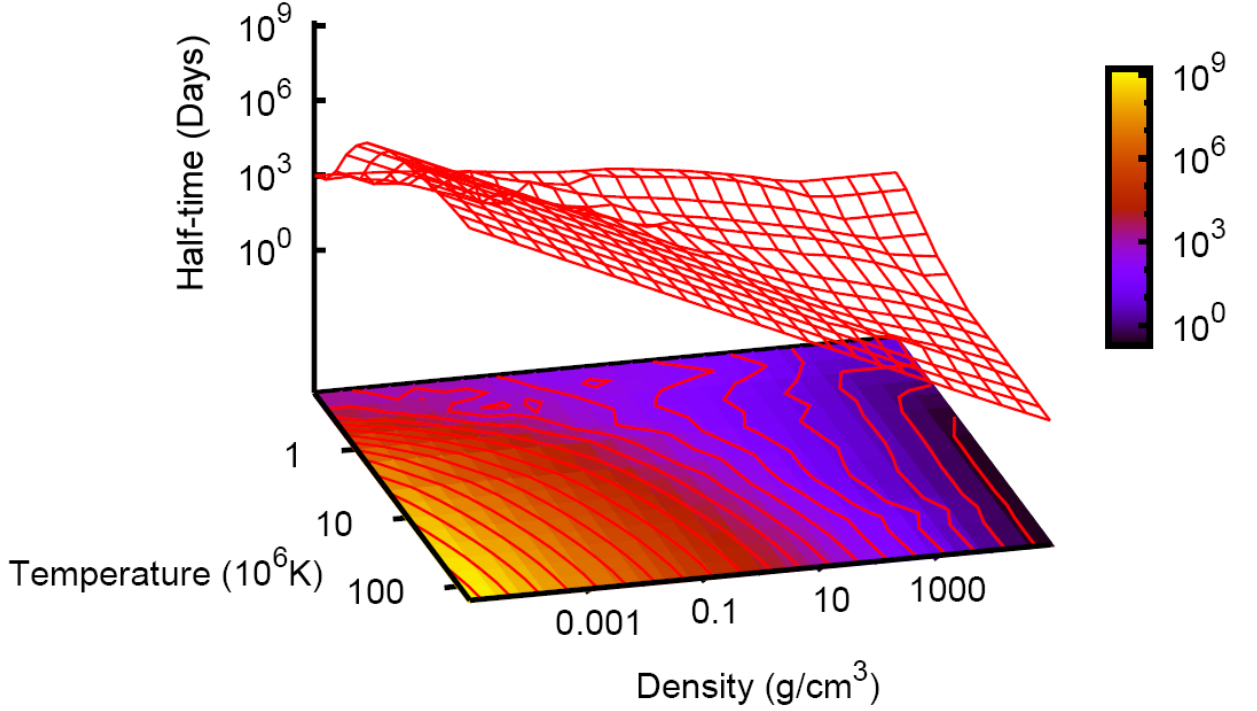


Fig. 1.— The electron-capture half-life in days for ${}^7\text{Be}$ as a function of ρ and T .

giving rise to the discrete part of the spectrum, the kinetic terms are left unprojected. In this way, as the eigenfunctions of the kinetic energy operator are plane waves at a given energy, one can “recover” the energy continuum. Furthermore, the sums over the discrete states n in Eq. (10) should be thought of as integrals over the continuum. In our case a $cc - pVDZ$ Gaussian basis set (GBS), centered on the ${}^7\text{Be}$ nucleus, has been optimized for the calculation of the bound states. We underline that the addition of the continuum states to the projected Coulomb interaction can have significant enhancement effects on the decay

Table 3		
	Energy	$\rho_{e\uparrow}(0)$
Hartree-Fock	-14.5729914739	17.68521
Full-CI	-14.6604710493	17.68060

Table 2: Energy of the isolated beryllium atom in atomic units and spin-up density at the nucleus obtained through the HF and CI calculations.

rate over a wide portion of the parameter space spanned. This however does not include the solar case, where our estimates are essentially indistinguishable from those reported by Adelberger et al. (2011). We notice in any case that, when applicable, our changes point to the opposite direction with respect to the suggestions by Shaviv & Shaviv (2003) for the Sun.

Our two-body scattering framework allows us to go beyond even the HF treatment of the screening; therefore, we estimated the importance of correlations by computing $\rho_e(0)$ for an isolated ${}^7\text{Be}$ atom using the Full Configuration Interaction approach (FCI) for the previously used $cc - pVDZ$ GBS. We did not find any appreciable difference between the $\rho_e(0)$ estimates calculated by the HF and by the FCI methods, up to the third digit (see Table 3), thus justifying our mean-field approach, which neglects dynamical correlations.

The calculation of the decay rate, performed at different T and ρ values using our approach is reported in Figure 1. We recall once again that the above treatment of the many-body interaction goes beyond the DH approximation previously used to estimate the electron-capture decay rate in the Sun (Iben et al. 1967; Bahcall 1962). The field of applicability of the HF screening effects can in fact be extended rigorously, to cover the whole range of parameters found in the layers between the H-burning region and the envelope base in evolved stars.

4. An application to the Li production and destruction in evolved stars

As an example of application of our new rate estimates to practical nucleosynthesis problems in stars, we briefly illustrate here the situation for rather low mass stars ($M \lesssim 2M_{\odot}$) of solar metallicity, undergoing the RGB and AGB evolutionary phases in presence of deep-mixing processes. They were recently discussed by Palmerini et al. (2011a,b) within the framework of reaction rates offered by Adelberger et al. (2011).

We consider here only the impact on the above astrophysical scenario of our "best choice" for the reaction rate (our new method), without analyzing the individual behavior of all the four estimates presented, as we are preparing a more thorough analysis on that, to appear in a forthcoming paper, also dealing with various stellar masses and compositions.

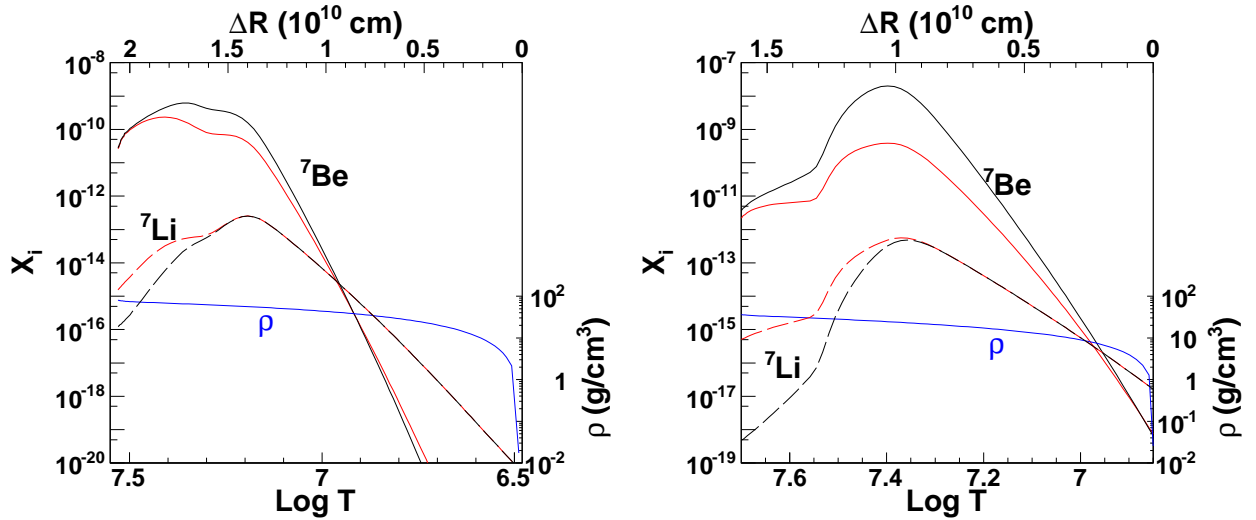


Fig. 2.— A comparison between the equilibrium abundances of ${}^7\text{Be}$ and ${}^7\text{Li}$ achieved in the layers above the H-burning shell, adopting our ${}^7\text{Be}$ life-time (red line) and the one extrapolated by Adelberger et al. (2011) (black line), in a $2 M_{\odot}$ evolved star of solar metallicity. Panel a) refers to typical RGB conditions, panel b) to AGB stages. The matter density is also shown (blue line), and is referred to the scale on the right axis.

Figure 2 (a,b) shows the abundances of ${}^7\text{Be}$ and of its daughter ${}^7\text{Li}$ in the layers below the convective envelope bottom and above the H-burning shell. They are plotted shortly

after the bump of the Luminosity Function on the RGB (panel a) and in between two thermal pulses, during quiet H-burning, on the AGB (panel b). The stellar models are the same discussed in Palmerini et al. (2011b). The red lines illustrate the situation obtained with our new rate (the case previously labelled HF), while the black line shows the previous findings, obtained with extrapolations from Adelberger et al. (2011), hence based on the DH approximation. The right-end limit of the plot, at the position $\Delta r = 0$, characterized by temperatures below 10^7K , represents the base of the envelope; the left-end limit is the region where the maximum energy is released from H-burning. As is shown, the matter density of the layers considered never achieves the high values typical of the solar core: this is the most critical reason why the DH approximation is inadequate for evolved stars. In our more general approach both higher and lower values of the electron density near the ${}^7\text{Be}$ nucleus can be found, depending on the conditions; however, over a major part of the region of interest, where the density is not far from one tenth solar and the temperature remains high enough ($T \gtrsim 10^7\text{ K}$) the values of $\rho_e(0)$ we find are higher than in the DH model; the electron captures are therefore faster than in Palmerini et al. (2011b), and a lower equilibrium abundance of ${}^7\text{Be}$ is established.

Notice that in our present example neither the ${}^3\text{He}+{}^4\text{He}$ rate, nor the ${}^7\text{Be}+\text{p}$ or the ${}^7\text{Li}+\text{p}$ rate have been modified, so that the variations shown in Figure 2 are entirely due to the new approach adopted in computing electron captures on ${}^7\text{Be}$. As discussed before, further effects are actually to be expected on proton captures, as the changes in the electron density will affect the screening of the Coulomb barrier for charged-particle interactions.

As discussed in the Section 1, it is known that interpreting the observed isotopic abundances of light and intermediate elements in evolved stars does not require only the use of the proper reaction rates, but also needs the assumption that deep mixing phenomena occur, both destroying fragile nuclei of the envelope (like Li), by exposing them to high

temperatures, and carrying to the surface products of H-burning nucleosynthesis. These mixing mechanisms are generally parameterized and depend on two main parameters; in the approach by Palmerini et al. (2011a,b) these parameters are the mass circulation rate (in units of $10^{-6} M_{\odot}/\text{yr}$) induced by the transport processes (\dot{M}_6) and the depth in the structure they achieve. This last is expressed in terms of the (logarithmic) temperature difference between the deepest mixed layers and those where the maximum energy is released in the H-shell ($\Delta = \log T_H - \log T_P$). (Recently, an analysis devised specifically for fixing such extra-mixing parameters, adopting bright RGB stars as constraints, was carried out by Abia et al. 2012, confirming the indications by Palmerini et al. on the need of a rather shallow and slow mixing on the RGB).

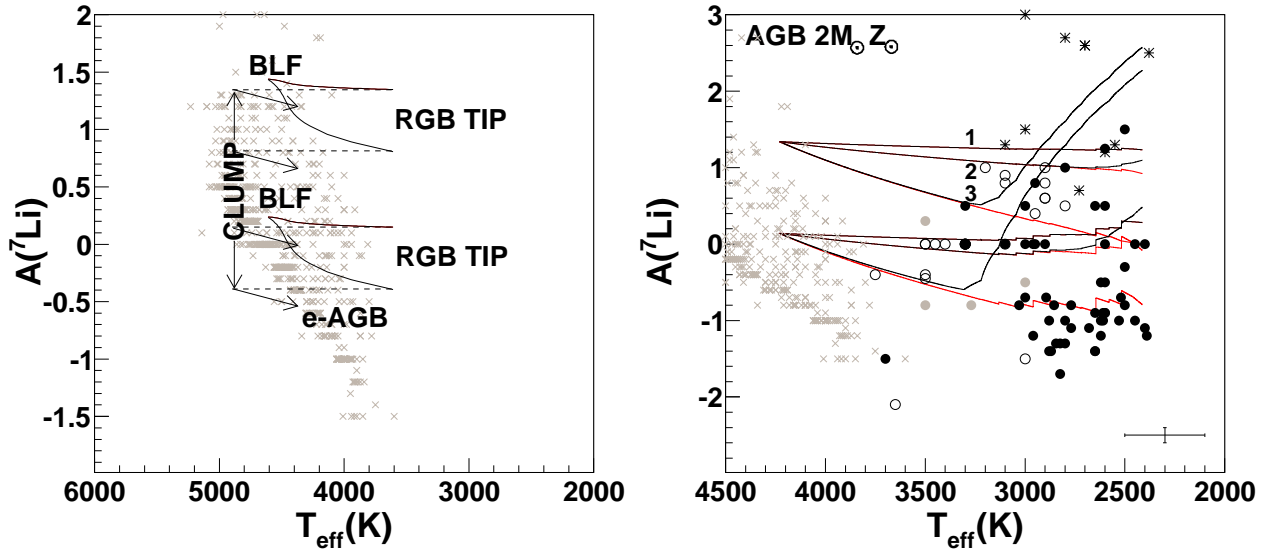


Fig. 3.— Panel a) The Li destruction induced by extra-mixing on the RGB. Panel b) The same effects for AGB stages (see text for explanations, and Palmerini et al. (2011b) for the details of the observational points and their references)

With reference to Panel a) in Figure 3, the points labeled BLF indicate the position in temperature of the Bump of the Luminosity Function, for two representative Li abundances, inside the wide spread allowed both by observations and models of the previous evolutionary

stages ($-0.3 \lesssim A(\text{Li}) \lesssim 1.5$); crosses indicate observations. From each one of the two BLF conditions chosen, the two black curves show the Li destruction induced by adopting, for the extra-mixing parameters, $\Delta = 0.22$ and $\dot{M}_6 = 0.01$ (upper curve) or 0.1 (lower curve). The effects of deep mixing are considered up to the moment when the RGB tip is reached. Subsequently, the temperature increases at constant values of $A(\text{Li})$ (dashed lines) up to the start of core He-burning (in the CLUMP region in the plot), after which Li would decrease again during the early-AGB stages (e-AGB in the plot; see also Palmerini et al. 2011b, for details). The curves showing the evolution of Li are completely insensitive to the adoption of the new or of the old rate for e^- -captures. Panel b) of Figure 3 shows instead that a different situation emerges during the subsequent AGB evolution. Here we started the computations from three initial values of the Li abundance, inside the observed spread left by RGB stages. Open and solid dots in the Figure represent observations of M-MS-S and of C(N) stars, respectively. Asterisks show the high Li abundances of CJ stars. The curves refer to stellar models with $\Delta = 0.22$ and $\dot{M}_6 = 0.1, 0.3, 1$ (cases labelled 1, 2, 3, respectively). The black curves are obtained using the ${}^7\text{Be} + e^-$ rate extrapolated by Adelberger et al. (2011), while the red ones refer to our best choice from the present paper (HF). It is clear that large changes emerge (in particular, with the new rate, Li production becomes impossible).

The reasons for the above dichotomy between RGB and AGB stages can be understood with reference to the time scales for ${}^7\text{Be}$ mixing and decay in the two cases. They are shown in Figure 4. As the figure shows, for the range of mixing rates required to explain the other RGB chemical anomalies (panel a) both the new and old choice for the ${}^7\text{Be}$ decay provide a short enough lifetime for ${}^7\text{Be}$, to allow its decay to Li before being saved to the envelope. In other words, conditions suitable for Be destruction are in any case met, both with the older and with the newer choice of the rate. This explains why the new estimate for the rate, which has evident effects in the stellar structure shown in panel a) of Fig 2, does not

modify the envelope abundances produced by the mixing process. The opposite occurs for AGB stages (panel b). Here, the reduction in the lifetime of ${}^7\text{Be}$ obtained with our new rate is strong enough that even with relatively fast mixing processes the destruction of Li in the envelope is not compensated, and the highest observed Li abundances (typical of CJ stars) cannot be reached. Essentially, with our rate Li behaves, on the AGB, in a way similar to what occurs on the RGB: destruction always prevails.

We notice that, far from creating a new problem, this finding is now in agreement with the indications provided by other chemical anomalies of the very peculiar CJ stars. Let’s comment on this in some more detail. In Palmerini et al. (2011b) it was surprisingly shown that, adopting the extrapolation to AGB conditions of the ${}^7\text{Be}$ lifetime from Adelberger et al. (2011), the high Li abundances observed in CJ-type carbon stars could be explained in the framework of the evolution of single stellar structures experiencing rather fast extra-mixing (see in particular Fig. 10 in Palmerini et al. 2011b). This result was in itself quite strange, as many peculiarities in such objects suggested instead, since a long time, that they do not follow the “normal” evolutionary sequence for LMS. This is in particular demonstrated by their luminosity, on average lower than for other C stars, by their lack of enrichment in s-process elements and by the fact that a remarkable fraction of CJ stars have O-rich shells. Among the hypotheses presented in the literature for explaining the anomalous CJ evolutionary path, binarity is probably the most commonly-invoked scenario (Lambert et al. 1990; Abia & Isern 2000), especially if leading to coalescence into a single peculiar object (McClure 1997). In this case, obviously, the high Li abundances of the peculiar descendants of such a stellar merging are not expected to be explained by single-star nucleosynthesis. We actually predict that Li destruction, with our new rate, be even more facilitated than what emerges from the first simple example of Figure 3. In fact a further effect is expected by an increase in the electron screening, due to the now higher (on average) electron densities near the nuclei, making proton captures on Li more effective.

In general, the Li-rich red giants (even outside the peculiar CJ class) need really exceptionally fast transport rates to explain the net Li production. Their small number says that these phenomena must be very rare, or concentrated in extremely short evolutionary stages.

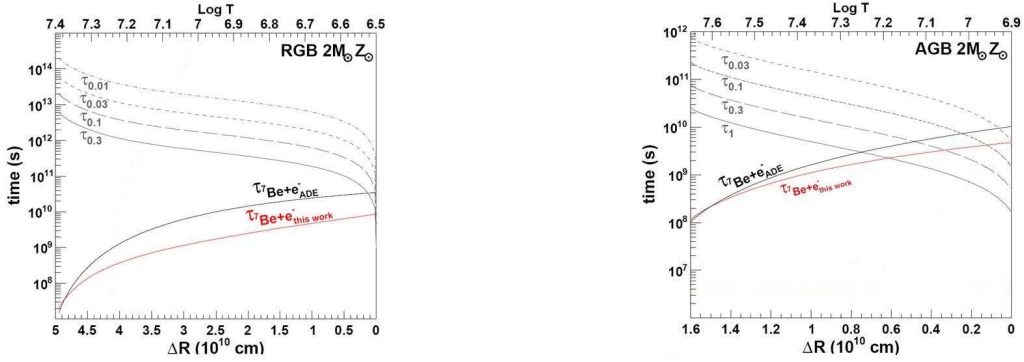


Fig. 4.— A comparison between our life-time for ${}^7\text{Be}$, $\tau_{\tau_{\text{Be}}}$ (red line) and the one extrapolated from Adelberger et al. (2011) (black line) with the time scales of non-convective mixing at various rates (labelled by the mixing rate in units of $10^{-6} M_{\odot}/\text{yr}$) in the radiative layers between the H-burning shell and the base of the convective envelope, for a star with $2 M_{\odot}$ and solar metallicity. Panel a) presents a typical situation for the RGB phase, while panel b) is instead typical of AGB conditions.

5. Conclusions

In this note we have presented a revision of the methods normally employed for estimating electron captures and, more in general, the electron density near a nucleus in a stellar plasma. For this scope we have devised an *ab-initio* technique, based on a formalism that goes beyond the previously-adopted ones. In our method, we firstly reduced the complicated many-body problem by a screened two-body scattering model, by using an “adiabatic” factorization of the eigenfunctions, resembling the Born-Oppenheimer (BO) approximation. We did that by fixing the reference frame into the ${}^7\text{Be}$ nucleus and then

writing the different parts of the Hamiltonian in this frame. The frame itself was considered as non-inertial, to account for the possibility that ${}^7\text{Be}$ be in motion in a rather complex way. In this coordinate transformation, the non-inertiality translated into some technical complicacy, with the need of considering the ensuing apparent forces. The mathematical details of this procedure were presented in an Appendix. In our Hamiltonian we then had to include the electron kinetic and the electron-Be potential energies, the proton kinetic and proton-Be potential energies, the Be kinetic energy, the electron-proton, electron-electron, proton-proton interactions. Furthermore, we also had to consider two-particle kinetic terms, which identify the coordinates of the j -electron and J -proton relative to the ${}^7\text{Be}$ coordinate. In particular, the conditions under which the two terms coupling the Be and plasma momenta must be considered carefully, as this is crucial for the application of our mean-field treatment. We then looked for separable eigensolutions and wrote the wavefunction factorization in a way different from the usual formulation of the BO approximation. Indeed, at variance with that approach, in our method there is neither the need that the electronic potential energy surfaces be widely separated, nor that there is a mass scale difference among the particles. By introducing the two-body framework and the relative coordinate system, we achieved two main results. The first one is that in our approach the ${}^7\text{Be}$ nucleus is free to move around (thus overcoming the limitations of the Born-Oppenheimer scheme); the second one is that the two-body electron- ${}^7\text{Be}$ density-matrix can be factorized as the product of two one-body density-matrices and thus it is possible to introduce different schemes of approximations to the many-body interaction, including the Hartree-Fock's one. Then, the screening effects due to all the fermions of the environment, which modify the electron- ${}^7\text{Be}$ scattering, were taken into account, using standard many-body techniques.

By comparing our results with those obtained at various levels of simplification of the theory we showed that, while the traditional DH approximation yields reliable results

for the solar core, where both high temperature and high density conditions exist, such simplified methods do not always hold in stellar evolution. In particular, in the low density and temperature environments characterizing partial H-burning above the H-shell in Red Giants, where lithium undergoes important depletion, we showed that our general method should be used and that extrapolations from existing e^- -capture rates on ${}^7\text{Be}$ in the Sun are not applicable.

As an example of the astrophysical consequences of our new method we recomputed, for a star of $M = 2M_{\odot}$ and solar metallicity, the evolution of the surface Li abundance in presence of deep mixing mechanisms. While, for RGB phases, with the new technique we re-obtain previously known results, on the AGB (where the density drops more remarkably) a stronger Li depletion was obtained and it was shown that high Li abundances (as observed e.g. in CJ-type carbon-rich giants) cannot be the result of extra-mixing occurring in single stars, but need more intricate evolutionary paths, as already speculated in the past from other chemical peculiarities of these objects.

Apart from the limited example presented in this first contribution, our method yields, in the regions characterized by temperatures of one to a few 10^7K and moderate densities (from 1 to 30-40 g/cm^3) higher values of the electron density at the nucleus than the DH approach. These conditions are not relevant for the solar core, but are important in red giant stars and in sub-envelope layers of MS stars. This should have the effect of enhancing, in those astrophysical environments, the electron screening, thus favoring thermonuclear fusion. Such a possibility may be especially important for light nuclei (like Li, or ${}^3\text{He}$), burning at relatively low temperature and that are related to crucial cosmological problems, like the explanation of the gradual ${}^3\text{He}$ consumption in the Universe and of the huge Li destruction below the surface of main sequence stars, including our Sun.

We thank Dr. G. Garberoglio (Bruno Kessler Foundation) for carefully reading

the manuscript and invaluable suggestions. ST gratefully acknowledges the Institute of Advanced Studies in Bologna for the logistic support provided during his fellowship. SP acknowledges support from the Spanish Grant AYA2011-22460

A. Transformation to relative coordinates

The calculation of the electron-capture decay rate in a many-body system is a difficult task, thus we propose to use an “adiabatic” approximation of the Hamiltonian, which resembles the widely used Born-Oppenheimer approach.

In order to derive the equation of motion for the fermions in the coordinate system relative to the ${}^7\text{Be}$ nucleus, we will consider a model system composed by a single ${}^7\text{Be}$ atom surrounded by N_p protons and N_e electrons. The Hamiltonian of such system in the laboratory frame can be written:

$$\begin{aligned}
 H = & -\frac{1}{2M_{\text{Be}}}\nabla_{\text{Be}}^2 + \sum_{j=1}^{N_e} \left(-\frac{1}{2m_e}\nabla_{e,j}^2 \right) + \sum_{J=1}^{N_p} \left(-\frac{1}{2m_p}\nabla_{p,J}^2 \right) - \sum_{j=1}^{N_e} \frac{Z_{\text{Be}}}{|\mathbf{R}_{\text{Be}} - \mathbf{r}_{e,j}|} \\
 & + \sum_{J=1}^{N_p} \frac{Z_{\text{Be}}}{|\mathbf{R}_{\text{Be}} - \mathbf{R}_{p,J}|} - \sum_{j=1}^{N_e} \sum_{J=1}^{N_p} \frac{1}{|\mathbf{r}_{e,j} - \mathbf{R}_{p,J}|} + \sum_{j=1}^{N_e} \sum_{k=j+1}^{N_e} \frac{1}{|\mathbf{r}_{e,j} - \mathbf{r}_{e,k}|} \\
 & + \sum_{J=1}^{N_p} \sum_{K=J+1}^{N_p} \frac{1}{|\mathbf{R}_{p,J} - \mathbf{R}_{p,K}|} \tag{A1}
 \end{aligned}$$

By performing the following transformation to the (${}^7\text{Be-}e^-$ and ${}^7\text{Be-}p^+$) relative coordinates

$$\begin{aligned}
 \mathbf{R}'_{\text{Be}} &= \mathbf{R}_{\text{Be}}, & \mathbf{r}'_{e,j} &= \mathbf{r}_{e,j} - \mathbf{R}_{\text{Be}}, & \mathbf{R}'_{p,J} &= \mathbf{R}_{p,J} - \mathbf{R}_{\text{Be}} \\
 \nabla_{\text{Be}} &= \nabla'_{\text{Be}} - \sum_{J=1}^{N_p} \nabla'_{p,J} - \sum_{j=1}^{N_e} \nabla'_{e,j}, & \nabla'_{e,j} &= \nabla_{e,j}, & \nabla'_{p,J} &= \nabla_{p,J} \tag{A2}
 \end{aligned}$$

one obtains:

$$\begin{aligned}
H = & \sum_{j=1}^{N_e} \left(-\frac{1}{2m_e} - \frac{1}{2M_{Be}} \right) \nabla'_{e,j}{}^2 + \sum_{J=1}^{N_p} \left(-\frac{1}{2m_p} - \frac{1}{2M_{Be}} \right) \nabla'_{p,J}{}^2 - \sum_{j=1}^{N_e} \frac{Z_{Be}}{|\mathbf{r}'_{e,j}|} + \sum_{J=1}^{N_p} \frac{Z_{Be}}{|\mathbf{R}'_{p,J}|} \\
& - \sum_{j=1}^{N_e} \sum_{J=1}^{N_p} \frac{1}{|\mathbf{r}'_{e,j} - \mathbf{R}'_{p,J}|} + \sum_{j=1}^{N_e} \sum_{k=j+1}^{N_e} \frac{1}{|\mathbf{r}'_{e,j} - \mathbf{r}'_{e,k}|} + \sum_{J=1}^{N_p} \sum_{K=J+1}^{N_p} \frac{1}{|\mathbf{R}'_{p,J} - \mathbf{R}'_{p,K}|} - \frac{1}{2M_{Be}} \nabla'_{Be}{}^2 \\
& - \sum_{\substack{J,J'=1 \\ J \neq J'}}^{N_p} \left(\frac{1}{M_{Be}} \nabla'_{p,J} \cdot \nabla'_{p,J'} \right) - \sum_{\substack{j,j'=1 \\ j \neq j'}}^{N_e} \left(\frac{1}{M_{Be}} \nabla'_{e,j} \cdot \nabla'_{e,j'} \right) - \frac{1}{M_{Be}} \sum_{j=1}^{N_e} \sum_{J=1}^{N_p} \nabla'_{p,J} \cdot \nabla'_{e,j} \\
& + \sum_{j=1}^{N_e} \left(\frac{1}{M_{Be}} \nabla'_{e,j} \cdot \nabla'_{Be} \right) + \sum_{J=1}^{N_p} \left(\frac{1}{M_{Be}} \nabla'_{p,J} \cdot \nabla'_{Be} \right)
\end{aligned} \tag{A3}$$

Within this model the ${}^7\text{Be}$ nucleus plays the role of the heavy nucleus in the BO approximation, moving more slowly than the light particles (electrons and protons).

Eq. (A3) can be simplified by neglecting all the inter-particle coupling terms, which are divided by the Be mass (M_{Be}). However, the last two terms in Eq. (A3) are special as they couple the Be nucleus and plasma momenta. Thus, we need to find the conditions under which these two coupling terms can be neglected as this is crucial for the application of our mean-field treatment. To determine when this is possible, one can notice that the two-body density-matrix of the system in relative coordinates at temperature T is given by:

$$\mathcal{Z} = \frac{1}{Z} \sum_{\alpha} \int \frac{d\mathbf{k}}{(2\pi)^3} e^{-\frac{E_{r,\alpha\mathbf{k}}}{k_B T}} e^{-\frac{1}{2M_{Be}} \frac{k^2}{k_B T}} |\Phi_{\alpha,\mathbf{k}} \rangle \langle \Phi_{\alpha,\mathbf{k}}| \otimes |\chi_{\mathbf{k}} \rangle \langle \chi_{\mathbf{k}}| \tag{A4}$$

where α identifies the electronic quantum numbers, $E_{r,\alpha\mathbf{k}}$ are the eigenvalues of the secular problem for Φ , and Z is the canonical partition function. The exponential term in Eq. (A4) kills the integral, unless:

$$k \sim \sqrt{2M_{Be}k_B T} \tag{A5}$$

Using Eq. (A5), the two coupling terms in Eq. (6) are of the order of $|\frac{1}{M_{Be}} \mathbf{k} \cdot \nabla'_{e,j}| \simeq 2\sqrt{k_B T K_e m_e / M_{Be}}$ and $|\frac{1}{M_{Be}} \mathbf{k} \cdot \nabla'_{p,j}| \simeq 2\sqrt{k_B T K_p m_p / M_{Be}}$, where K_e and K_p are the

electron and proton kinetic energies, respectively. Therefore, if the two conditions

$$4k_B T m_e / M_{Be} \ll K_e, \quad 4k_B T m_p / M_{Be} \ll K_p \quad (\text{A6})$$

hold, then $\left(-\frac{i}{m_e} \mathbf{k} \cdot \nabla'_{e,j}\right)$ and $\left(-\frac{i}{m_p} \mathbf{k} \cdot \nabla'_{p,j}\right)$ are negligible. These conditions are generally satisfied, due the presence of the Be mass in the denominator and to the fact that the scalar products $\left(-\frac{i}{m_e} \mathbf{k} \cdot \nabla'_{e,j}\right)$ and $\left(-\frac{i}{m_p} \mathbf{k} \cdot \nabla'_{p,j}\right)$ contain the cosine of the reciprocal direction of the two multiplying vectors, which, on average, is very small. Finally, the last three terms of the Hamiltonian (A3) can be safely neglected as they contain a multiplying factor proportional to the inverse of the Be mass.

B. The Thomas–Fermi and Debye–Hückel models

The widely used DH model can be obtained via a two-step approximation starting from the TF theory of the electron gas. The TF model is a simplified HF theory, in which the electron gas is treated within the local density approximation (LDA), so that a large number of electrons is needed in a region where the potential is nearly constant. In this theory the density is thus diagonal in the electron coordinates:

$$\rho_{j,\alpha\alpha'}(\mathbf{r}, \mathbf{r}') = \rho_{j,\alpha\alpha'}(\mathbf{r}) \delta(\mathbf{r} - \mathbf{r}') \quad (\text{B1})$$

$$\rho_{j,\alpha\alpha'}(\mathbf{r}) = \int \frac{d\mathbf{p}}{(2\pi)^3} \frac{\psi_{j,\alpha\mathbf{p}} \psi_{j,\alpha'\mathbf{p}}}{e^{\epsilon_{j,\mathbf{p}}} + 1} \quad (\text{B2})$$

and can be obtained by the self-consistent solution of the TF equation:

$$-\frac{p_j^2}{2m_j} \psi_{j,\alpha\mathbf{p}} + V_{j,\mathbf{p}}^{ext}(\mathbf{r}) \psi_{j,\alpha\mathbf{p}} - \mu_j \psi_{j,\alpha\mathbf{p}} + \sum_{\beta} V_{j,\alpha\mathbf{p}\beta\mathbf{p}}^{HF} \psi_{j,\beta\mathbf{p}} = \epsilon_{j,\mathbf{p}} \psi_{j,\alpha\mathbf{p}} \quad (\text{B3})$$

where $V_{j,\mathbf{p}}^{ext}(\mathbf{r})$ is the electron-nucleus interaction, μ is the chemical potential, α, α' identify the electron quantum numbers and

$$V_{j,\alpha\alpha'}^{HF}(\mathbf{r}, \mathbf{r}') = \delta(\mathbf{r} - \mathbf{r}') \sum_{j'\beta\beta'} \int d\mathbf{s} g_{j\alpha\beta,j'\alpha'\beta'}(\mathbf{r} - \mathbf{s}) \rho_{j',\beta\beta'}(\mathbf{s}, \mathbf{s}) - \sum_{\beta\beta'} g_{j\alpha\beta,j\beta'\alpha'}(\mathbf{r} - \mathbf{r}') \rho_{j,\beta\beta'}(\mathbf{r}, \mathbf{r}') \quad (\text{B4})$$

. Here g is the bare Coulomb potential.

In order to obtain the DH approximation, in the first step one substitutes the quantum-mechanical Fermi-Dirac statistics with the classical Boltzmann distribution, while, in a second step, the high-temperature (weak coupling) limit is obtained by Taylor expanding at the first order the exponential distribution:

$$\rho_j(\mathbf{r}) = \int \frac{d\mathbf{p}}{(2\pi)^3} e^{-\beta \left[\frac{p_j^2}{2m_j} + q_j \Phi(\mathbf{r}) - \mu_j \right]} \quad (\text{B5})$$

In this way one obtains the DH equation for a neutral plasma as follows:

$$\nabla^2 \Phi = \lambda_D \Phi \quad (\text{B6})$$

where

$$\Phi(\mathbf{r}) = \sum_{j'} \int d\mathbf{r}' \frac{q_{j'} \rho_{j'}(\mathbf{r}')}{|\mathbf{r} - \mathbf{r}'|}$$

In Eq. (B6), the DH length is defined by $\lambda_D = (\epsilon_r \epsilon_0 k_B T / \sum_{j=1}^N \rho_j^0 q_j^2)^{\frac{1}{2}}$, where k_B is the Boltzmann constant, ρ_j^0 is the mean charge density of the species j , ϵ_r and ϵ_0 are the relative and vacuum dielectric constants. In this framework, λ_D sets the characteristic length scale for the variation of the potential and of the charge concentration.

Acknowledgements. We are grateful to an unknown referee for very pertinent and helpful comments, which we believe were crucial for improving the quality of the presentation.

REFERENCES

- Abia, C., & Isern, J. 2000, ApJ 536, 448
- Abia, C., Palmerini, S., Busso, M., & Cristallo, S. 2012, A&A (in press), arXiv1210.1160A
- Adelberger, E.G., Garc a, A., Robertson, R.G.H. *et al.* 2011, Rev. Mod. Phys. 83, 195
- Alib s, A., Labay, J., & Canal, R. 2002, ApJ 571, 326
- Andrews, A.D., Rodon , M., Linsky, J.L. *et al.* 1988, A&A 204, 177
- M. Asplund, N. Grevesse, J. Sauval, and P. Scott ARA&A 47, 481 (2009).
- Bahcall J.N. 1962, Phys. Rev. 126, 1143
- Bahcall, J.N. & Moeller, C.P. 1969, ApJ 155, 511
- Balachandran, S. 1995, ApJ 446, 203
- Boesgaard, A.M., Deliyannis, C.P., Stephens, A., & Lambert, D.L. ApJ 492, 727 (1998).
- Boesgaard, A.M. 2005, *Cosmic Abundances as Records of Stellar Evolution and Nucleosynthesis*, ed. T. G. Barnes, III & F. N. Bash (San Francisco, CA:ASPC) 336, 39
- Boesgaard, A.M. & Tripicco, M.J. 1986a, ApJ 302, L49
- Boesgaard, A.M. & Tripicco, M.J. 1986b, ApJ 303, 724
- Bonifacio; P., Sbordone, L., Caffau, E. *et al.* , 2012, A&A 542, 87
- Brown, J.A. 1987, ApJ 317, 701
- Brown, L.S. & Sawyer, R.F. 1997, ApJ 489, 968

- Busso, M. 2011 In *Astronomy with Radioactivities*, ed. R. Diehl, D. H. Hartmann, & N. Prantzos, LNP, Berlin: Springer, 812, 309
- Busso, M., Gallino, R., & Wasserburg, G.J. 2003, PASA 20, 356
- Busso, M., Wasserburg, G.J., Nollett, K.M., & Calandra, A. 2007, ApJ 671, 802
- Casuso, E., & Beckmann, J.E. 2003, PASJ 55, 247
- Charbonnel, C. & Balachandran, S. 2000, A&A 359, 562
- Charbonnel, C. & Lagarde, N. 2010, A&A 522, 10
- Coc, A., & Vangioni, E. 2010, J Phys. Conf. Ser. 202, 012001
- D'Antona, F. & Ventura, P. 2010, in "Light elements in the Universe", IAU Symposium 268, p.395
- Debye, P. & Hückel, E. 1923, Phys. Z. 24, 185
- Denissenkov, P.A., Pinsonneault, M., & MacGregor, K.B. 2009, ApJ 696, 1823
- Eggenberger, P., Meynet, G., Maeder, A, *et al.* 2010, A&A 519, 116
- Emery, G.T. 1972, Ann. Rev. Nucl. Sci. 22, 165
- Fields, B.D., Olive, K.A., & Schramm, D.N. 1994, ApJ 435 185
- Fowler, C.M.R. 2005, *The Solid Earth: an Introduction to Global Geophysics*, (Cambridge: Cambridge University Press).
- Fowler, W.A., Caughlan, G.R., & Zimmerman, B.A. 1975, ARA&A 13, 69
- Fuller, G. M. & Smith, C. J. 2010, Phys. Rev. D 82, 125017
- Gruzinov, A.V. & Bahcall, J.N. 1997, ApJ 490, 437

- Hahn, H.P., Born, H.J. & Kim, J.I. 1976, *Radiochim. Acta* 23, 23
- Iben I.Jr., Kalata, K., & Schwartz, J. 1967, *ApJ* 150, 1001
- Johnson, C.W., Kolbe, E., Koonin, S.E., & Langanke, K. 1992, *ApJ* 392, 320
- Kumar, B.Y., Reddy, B.E. & Lambert, D.L. 2011, *ApJ* 730, L12
- Lambert, D.L., Hinkle, K.H., & Smith, V.V. 1990, *AJ* 99, 1612
- Lebzelter, T., Uttenthaler, S., Busso, M., Schultheis, M., & Aringer, B. 2012, *A&A* 538, L36
- Lee, K.K.M., & Steinle-Neumann, G. 2008, *Earth Plan. Sci. Lett.* 267, 628
- Maiorca, E., Magrini, L., Busso, M., Palmerini, S., & Trippella, O. 2012, *ApJ* 747, 53
- Mathews, G. J., Haight, R.C., Lanier, R. G. and White R.M. 1983, *Phys. Rev. C*, 28 879
- McClure, R.D. 1997, *PASP* 109, 256
- Michaud, G. 1986, *ApJ* 302, 650
- Michaud, G. & Charbonneau, P. 1991, *Space Sci Rev* 57, 1
- Morisato, T., Ohno, K., Ohtsuki, T., Hirose, Sluiter, M. & Kawazoe, Y. 2008, *PRB* 78, 125416
- Nordhaus, J., Busso, M., Wasserburg, G.J., Blackman, E.G., & Palmerini, S. 2008, *ApJ* 684, 29
- Ohtsuki, T., Ohno, K., Morisato, T., Mitsugashira, T., Hirose, K., Yuki, H. & Kasagi, J. 2007, *PRL* 98, 252501
- Palmerini, S., La Cognata, M., Cristallo, S. & Busso, M. 2011 *ApJ* 729, 3
- Palmerini, S., Cristallo, S., Busso, M. *et al.* 2011, *ApJ* 741, 26

- Pinsonneault, M. 1997, *ARA&A* 35, 557
- Pollack, H.N., Hurter, S.J. & Johnson, J.R. 1993 *Rev. Geophys.* 31, 267
- Quarati, P., & Scarfone, A.M. *J. Phys. G* 36, 025203
- Ray, A., Das, P., Saha, S.K., & Das, S.K. 2002, *Phys. Lett. B* 531, 187
- Sawyer, R.F. 2011, *Phys. Rev. C* 83, 5804
- Sestito, P., Degl’Innocenti, S., Prada Moroni, P.G., & Randich, S. 2006, *A&A* 454, 311
- Shaviv, N.J. & Shaviv, G. 2001, *MNRAS* 341, 119
- Spite, F. & Spite, M. 1982, *A&A* 115, 357
- Taioli, S., Simonucci, S. & Dapor, M. 2009, *Comput. Sci. Disc.* 2, 015002
- Taioli, S., Simonucci, S., Calliari, L., Filippi, M. & Dapor, M. 2009, *PRB* 79, 085432
- Taioli, S., Simonucci, S., Calliari, L., & Dapor, M. 2010, *Phys. Rep.* 493, 237
- Tilley, D.R. et al. 2002, *Nucl. Phys. A* 708, 163
- Uttenthaler, S. & Lebzelter, T. 2010 *A&A* 510, 62

Table 2

ρ (g/cm^3)	T ($10^6 K$)	λ_{Debye} <i>a.u.</i>	$\lambda_{De Broglie}$ ($e - p$)	$\rho_{HF}(0)$ <i>a.u.</i>	$\rho_{TF}(0)$	$\rho_B(0)$	$\rho_{DH}(0)$
1000.	1.	0.038	1.409 - 0.0329	71.87 ÷ 71.97	68.99 ÷ 69.11	42.61 ÷ 42.74	47.46 ÷ 47.55
100.		0.119		33.52 ÷ 33.53	29.53 ÷ 29.55	4.027 ÷ 4.031	19.13 ÷ 19.14
10.		0.377		17.37 ÷ 17.37	13.83 ÷ 13.83	0.945 ÷ 0.945	13.33 ÷ 13.33
1.		1.193		7.839 ÷ 7.837	5.708 ÷ 5.707	0.184 ÷ 0.184	8.151 ÷ 8.149
0.1		3.771		1.940 ÷ 1.940	1.415 ÷ 1.415	0.044 ÷ 0.044	2.059 ÷ 2.058
0.01		11.93		0.278 ÷ 0.278	0.220 ÷ 0.220	0.0075 ÷ 0.0075	0.279 ÷ 0.279
0.001		37.71		0.0308 ÷ 0.0308	0.0264 ÷ 0.264	0.0012 ÷ 0.0012	0.0303 ÷ 0.303
1000.		10.		0.119	0.445 - 0.0103	122.43 ÷ 122.89	116.21 ÷ 116.68
100.	0.377		20.23 ÷ 20.27	19.53 ÷ 19.57		10.36 ÷ 10.39	19.54 ÷ 19.58
10.	1.193		2.578 ÷ 2.581	2.554 ÷ 2.558		2.515 ÷ 2.519	2.570 ÷ 2.573
1.	3.771		0.274 ÷ 0.275	0.274 ÷ 0.275		0.274 ÷ 0.274	0.274 ÷ 0.275
0.1	11.93		0.0281 ÷ 0.0282	0.0281 ÷ 0.0282		0.0281 ÷ 0.0282	0.0281 ÷ 0.0281
0.01	37.71		$(2.84 \div 2.84) \cdot 10^{-3}$	$(2.84 \div 2.84) \cdot 10^{-3}$		$(2.84 \div 2.84) \cdot 10^{-3}$	$(2.83 \div 2.83) \cdot 10^{-3}$
0.001	119.3		$(2.84 \div 2.84) \cdot 10^{-4}$	$(2.84 \div 2.84) \cdot 10^{-4}$		$(2.84 \div 2.84) \cdot 10^{-4}$	$(2.84 \div 2.84) \cdot 10^{-4}$
1000.	100.		0.377	0.141 - 0.0033		78.31 ÷ 80.39	78.24 ÷ 80.32
100.		1.193	9.051 ÷ 9.289		9.051 ÷ 9.288	9.031 ÷ 9.268	9.051 ÷ 9.288
10.		3.771	0.773 ÷ 0.787		0.773 ÷ 0.787	0.773 ÷ 0.787	0.773 ÷ 0.787
1.		11.93	0.0775 ÷ 0.0789		0.0775 ÷ 0.0789	0.0775 ÷ 0.0789	0.0775 ÷ 0.0789
0.1		37.71	$(7.75 \div 7.90) \cdot 10^{-3}$		$(7.75 \div 7.90) \cdot 10^{-3}$	$(7.75 \div 7.90) \cdot 10^{-3}$	$(7.75 \div 7.90) \cdot 10^{-3}$
0.01		119.3	$(7.75 \div 7.90) \cdot 10^{-4}$		$(7.75 \div 7.90) \cdot 10^{-4}$	$(7.75 \div 7.90) \cdot 10^{-4}$	$(7.75 \div 7.90) \cdot 10^{-4}$
0.001		377.1	$(7.75 \div 7.90) \cdot 10^{-5}$		$(7.75 \div 7.90) \cdot 10^{-5}$	$(7.75 \div 7.90) \cdot 10^{-5}$	$(7.75 \div 7.90) \cdot 10^{-5}$

Values of the electron density $\rho_e(0)$ (in atomic units) at the Be nucleus, for different theoretical approaches (see text for explanations)